

$[(\text{CH}_3)_3\text{NCH}_2\text{CH}_2\text{NH}_3]\text{SnI}_4$: A Layered Perovskite with Quaternary/Primary Ammonium Dications and Short Interlayer Iodine–Iodine Contacts

Zhengtao Xu, David B. Mitzi,* and David R. Medeiros

IBM T. J. Watson Research Center, P.O. Box 218, Yorktown Heights, New York 10598

Received November 20, 2002

The organic–inorganic hybrid $[(\text{CH}_3)_3\text{NCH}_2\text{CH}_2\text{NH}_3]\text{SnI}_4$ presents a layered perovskite structure, templated by an organic dication containing both a primary and a quaternary ammonium group. Due to the high charge density and small size of the organic cation, the separation of the perovskite layers is small and short iodine–iodine contacts of 4.19 Å are formed between the layers. Optical thin-film measurements on this compound indicate a significant red shift of the exciton peak (630 nm) associated with the band gap, as compared with other SnI_4^{2-} -based layered perovskite structures.

Organic–inorganic perovskites¹ such as $(\text{RNH}_3)_2\text{MX}_4$ and $(\text{H}_3\text{NRNH}_3)\text{MX}_4$ (M = divalent metal; X = halogen atoms; R = organic moiety) are widely studied hybrid crystalline systems that exhibit interesting magnetic,^{2–6} optical,^{7–10} and electrical^{11–13} properties. The inorganic components in these systems usually consist of extended anionic networks of corner-sharing metal halide octahedra (e.g., SnX_6 , PbX_6 , CdX_6 etc), whereas the organic molecules contain positively charged groups such as ammonium or formamidinium, which serve to counterbalance the charge on the inorganic framework and template the inorganic layers. Our lab has been interested in the layered tin(II) iodide based systems partly because of the highly tunable electronic structure of the semiconducting inorganic sheets. Past studies have shown that the band gap can be modified by controlling the

thickness of the inorganic layer,^{12–15} by making substitutions on either the metal or halogen site,^{9,10,14} or by selecting different organic cations.^{16,17} Among the diverse systems studied, two common features are observed: (1) the organic cations generally contain strong hydrogen donors such as the primary ammonium RNH_3^+ (R = organic groups), the formamidinium $[\text{H}_2\text{N}=\text{C}(\text{R})\text{NH}_2]^+$ (R = iodo^{12,18} or organic groups^{19,20}), or the recently reported imidazolium groups,²¹ which interact with the inorganic layer through electrostatic hydrogen bonding; (2) the 2-D inorganic layers are usually well separated by the organic molecules. Although significant $\text{X}\cdots\text{X}$ (X = Br, Cl) interactions were observed among the inorganic layers in copper(II) halide layered perovskites,^{4,22} interlayer interactions found in layered perovskites based on group 14 (IV A) metal halides have generally been much weaker, with reported^{21,23} shortest $\text{I}\cdots\text{I}$ contacts (>4.42 Å) being significantly longer than the van der Waals distance (4.0 Å²⁴).

Here we report a layered perovskite based on tin(II) iodide that is noteworthy in both the organic cation and the interlayer interaction. First, it is templated simultaneously by a quaternary ammonium group as well as the traditional primary ammonium group, leading to weaker hydrogen bonding between the organic cation and the inorganic framework. Second, the single-crystal structure reveals more intimate iodine–iodine contacts across the perovskite layers, suggesting enhanced interaction between the layers. In addition, optical absorption experiments on this compound reveal a substantial shift of the exciton state associated with the band gap toward longer wavelength (lower energy),

- (1) For a recent review, see: Mitzi, D. B. *Prog. Inorg. Chem.* **1999**, *48*, 1.
- (2) De Jongh, L. J.; Botterman, A. C.; De Boer, F. R.; Miedema, A. R. *J. Appl. Phys.* **1969**, *40*, 1363.
- (3) De Jongh, L. J.; Miedema, A. R. *Adv. Phys.* **1974**, *23*, 1.
- (4) Willett, R. D.; Place, H.; Middleton, M. *J. Am. Chem. Soc.* **1988**, *110*, 8639.
- (5) Long, G. S.; Wei, M.; Willett, R. D. *Inorg. Chem.* **1997**, *36*, 3102.
- (6) Sekine, T.; Okuno, T.; Awaga, K. *Inorg. Chem.* **1998**, *37*, 2129.
- (7) Xu, C.; Kondo, T.; Sakakura, H.; Kumata, K.; Takahashi, Y.; Ito, R. *Solid State Commun.* **1991**, *79*, 245.
- (8) Hong, X.; Ishihara, T.; Nurmikko, A. V. *Phys. Rev. B: Condens. Matter* **1992**, *45*, 6961.
- (9) Mitzi, D. B. *Chem. Mater.* **1996**, *8*, 791.
- (10) Papavassiliou, G. C. *Prog. Solid State Chem.* **1997**, *25*, 125.
- (11) Kagan, C. R.; Mitzi, D. B.; Dimitrakopoulos, C. D. *Science* **1999**, *286*, 945.
- (12) Mitzi, D. B.; Wang, S.; Feild, C. A.; Chess, C. A.; Guloy, A. M. *Science* **1995**, *267*, 1473.
- (13) Mitzi, D. B.; Feild, C. A.; Harrison, W. T. A.; Guloy, A. M. *Nature* **1994**, *369*, 467.

- (14) Calabrese, J.; Jones, N. L.; Harlow, R. L.; Herron, N.; Thorn, D. L.; Wang, Y. *J. Am. Chem. Soc.* **1991**, *113*, 2328.
- (15) Mitzi, D. B. *J. Chem. Soc., Dalton Trans.* **2001**, 1.
- (16) Mitzi, D. B.; Dimitrakopoulos, C. D.; Kosbar, L. L. *Chem. Mater.* **2001**, *13*, 3728.
- (17) Xu, Z.; Mitzi, D. B.; Dimitrakopoulos, C. D.; Maxey, K. R. *Inorg. Chem.*, in press.
- (18) Wang, S.; Mitzi, D. B.; Feild, C. A.; Guloy, A. *J. Am. Chem. Soc.* **1995**, *117*, 5297.
- (19) Papavassiliou, G. C.; Mousdis, G. A.; Koutselas, I. B. *Adv. Mater. Opt. Electron.* **1999**, *9*, 265.
- (20) Papavassiliou, G. C.; Mousdis, G. A.; Koutselas, I. B. *Z. Naturforsch.* **2001**, *56b*, 57.
- (21) Tang, Z.; Guan, J.; Guloy, A. M. *J. Mater. Chem.* **2001**, *11*, 479.
- (22) Halvorson, K.; Willet, R. D. *Acta Crystallogr., Sect. C* **1988**, *44*, 2071.
- (23) Guan, J.; Tang, Z.; Guloy, A. M. *Chem. Commun.* **1999**, 1833.
- (24) Bondi, A. *J. Phys. Chem.* **1964**, *68*, 441.

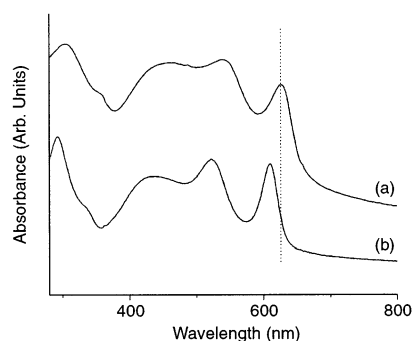


Figure 1. Room-temperature UV–vis absorption spectra for thin films of (a) **1** and (b) $(\text{PEA})_2\text{SnI}_4$. The dotted lines highlight the shifts in the peak positions. Thin films for both samples were made using similar procedures as described in the text (see Figures S1 and S2 in Supporting Information for X-ray diffraction scans of the thin film samples).

compared with other SnI_4 -based layered perovskites. The narrower band gap appears to be associated with the interlayer $\text{I}\cdots\text{I}$ contacts (which enhances the orbital interactions across the perovskite sheets), as well as other bonding features within the perovskite sheet, as will be mentioned below.

The compound $[(\text{CH}_3)_3\text{NCH}_2\text{CH}_2\text{NH}_3]\text{SnI}_4$ (**1**) was formed²⁵ by evaporating a methanol/acetonitrile solution containing tin(II) iodide (SnI_2) and 2-trimethylammonioethylammonium (TMAEA) diiodide $[(\text{CH}_3)_3\text{NCH}_2\text{CH}_2\text{NH}_3]\text{I}_2$. The crystals thus obtained are black in the bulk, but under a microscope (in transmission mode) appear to be platelets with a dark red tinge. Thin films of **1** for optical absorption measurements were deposited from a DMF solution onto a glass slide using a modified drop-casting method.²⁶ The optical absorption spectrum (Figure 1) features an exciton peak at 630 nm (1.97 eV), a significant shift to lower energy as compared with that (610 nm, 2.03 eV) of the well-known $(\text{PEA})_2\text{SnI}_4$ system (PEA: phenethylammonium).²⁷ The corresponding band edge of **1** is similarly shifted to lower energy.

The crystal structure²⁸ of **1** contains perovskite-like slabs of corner-sharing SnI_6 octahedra, alternating with TMAEA organic cation layers (Figure 2). The inorganic layers closely approach one another, resulting in a short distance of 4.19

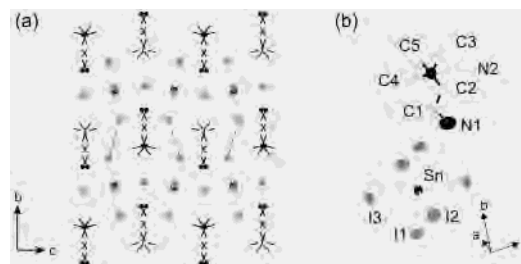


Figure 2. Crystal structure of **1**: (a) Viewed along the a axis; I, large gray spheres; Sn, large black spheres (partly eclipsed by I atoms); C, small open spheres; N, small black spheres. Dashed lines show the $\text{I}\cdots\text{I}$ contacts. For clarity, disordering of the $(\text{CH}_3)_3\text{N}$ group is omitted. (b) Thermal ellipsoids (50% probability) and atom labeling for the SnI_6 octahedron and the organic cation.

Å (van der Waals distance: 4.0 \AA^{24}) between the apical iodine atoms from neighboring layers. In comparison to the typical semiconducting layered perovskites, the iodine–iodine contacts between the layers impart a certain three-dimensional character to the current structure.¹⁰ The short iodine–iodine contacts, together with the two square-like units from the adjacent inorganic sheets, form cavities in which the TMAEA organic cation is enclathrated (Figure 3). Notably, the structural information encoded in the templating cation is well relayed onto the shape of the cavities formed by the host framework. As can be seen from Figure 3, the four apical Sn–I bonds on one side of the cavity point slightly outward, so as to open up the space for accommodating the bulky trimethylammonio group. On the side where sits the slender primary ammonium group, however, the four Sn–I bonds point inward, forming the

(25) Inside a nitrogen-filled drybox, tin(II) iodide (36 mg, 0.10 mmol) and 2-trimethylammonioethylammonium diiodide (37 mg, 0.10 mmol) were loaded in a vial and mixed with methanol (anhydrous, 6.0 mL) and acetonitrile (anhydrous, 4.0 mL). A transparent yellow solution was obtained after stirring for 2 h, which was then passed through a Teflon filter (pore size: $0.2 \mu\text{m}$). The filtrate was collected in an uncapped vial, and the solvents were allowed to evaporate at room temperature. Chunky, black crystals of **1** (suitable for single-crystal X-ray study) were formed over 2 or 3 days. The yield of **1** was nearly quantitative, with a small amount of yellow powder formed as a side product, which was readily separated by hand from the crystals of **1**. A powder sample of **1** showed an X-ray diffraction pattern consistent with the single crystal structure. The solid is moderately sensitive to air exposure (see Figures S2 and S3 in Supporting Information). It exhibited negligible solubility in solvents such as benzene, toluene, dichloromethane, and THF (tetrahydrofuran), but readily dissolved in DMF (N,N -dimethylformamide). ^1H NMR (400 MHz, DMF- d_7): δ 8.65 (s, broad, 3H), 4.11–4.07 (m, 2H), 3.90–3.86 (m, 2H), 3.54 (s, 9H). ^{13}C NMR (100 MHz, DMF- d_7): δ 62.5, 53.9, 34.4. Chemical analysis of the product $\text{C}_5\text{H}_{16}\text{N}_2\text{SnI}_4$: calcd [C (8.22%), H (2.21%), N (3.83%)]; found [C (8.28%), H (2.18%), N (3.84%)]. DSC (differential scanning calorimetry), TGA (thermogravimetric analysis) and melting experiments (all done in nitrogen atmosphere) indicated an onset of decomposition at $245 \text{ }^\circ\text{C}$ (corresponding to a transformation into a yellow powder), with melting noted above $255 \text{ }^\circ\text{C}$.

(26) After failing to obtain films of the desired phase from various spin coating and vapor-phase deposition attempts (for a review on methods for depositing thin films of hybrid materials, see: Mitzi, D. B. *Chem. Mater.* **2001**, *13*, 3283), we found that the following drop casting method provided thin films good enough for optical measurements. In a nitrogen-filled glovebox, compound **1** (12.0 mg) was dissolved in DMF (0.3 mL) to give a clear, yellow solution. Three or four drops of the solution were added onto a glass plate heated to $155 \text{ }^\circ\text{C}$. A small puddle (ca. 1 cm^2) was formed and the solvent evaporated rapidly; within a minute, black solid began to deposit around the puddle, and a piece of Kapton sheet (ca. $3 \times 3 \text{ cm}$) was immediately placed onto the glass plate to evenly spread the remaining solution. The Kapton sheet was then peeled off from the glass slide at a steady pace over 2–3 s. A dark red film was at once formed on the glass slide, which was maintained at $155 \text{ }^\circ\text{C}$ for another 2 min for the purpose of annealing and removal of residual solvent. An X-ray scan of the resultant film confirmed the formation of **1** (see Figure S2 in Supporting Information for more details). The films were highly crystallographically oriented with respect to the substrate, like hybrid films deposited using more traditional techniques (e.g., spin coating or thermal ablation).

(27) Papavassiliou, G. C.; Koutselas, I. B.; Terzis, A.; Whangbo, M.-H. *Solid State Commun.* **1994**, *91*, 695.

(28) The X-ray diffraction data for **1** were collected at room temperature from a crystal (platelet, $0.40 \text{ mm} \times 0.20 \text{ mm} \times 0.04 \text{ mm}$) on a Bruker SMART CCD diffractometer, equipped with a normal focus 2.4 kW sealed tube X-ray source (Mo $K\alpha$ radiation). The structure was solved by direct methods in $Cmca$ and refined on F^2 (full matrix, absorption corrections with SADABS) using the Shelxl 97 package. Hydrogen atoms were not located from the Fourier map, and all the non-hydrogen atoms were refined anisotropically. Except for the terminal carbon atoms on the trimethylammonio group, which are disordered over two sets of positions related by a mirror symmetry, no disordering is observed in the other atoms. Crystal data: orthorhombic, $Cmca$, $a = 12.602(1) \text{ \AA}$, $b = 20.257(2) \text{ \AA}$, and $c = 12.505(1) \text{ \AA}$, $V = 3192.2(4) \text{ \AA}^3$, $Z = 8$, $\mu = 93.07 \text{ cm}^{-1}$, $d_{\text{calcd}} = 3.040 \text{ g/cm}^3$, $R_{\text{int}} = 3.52\%$, $R1/wR2 = 3.85/10.97\%$ for 1927 unique observed reflections [$I \geq 2\sigma(I)$] and 76 variables ($R1/wR2 = 4.61/11.44\%$ for all data).

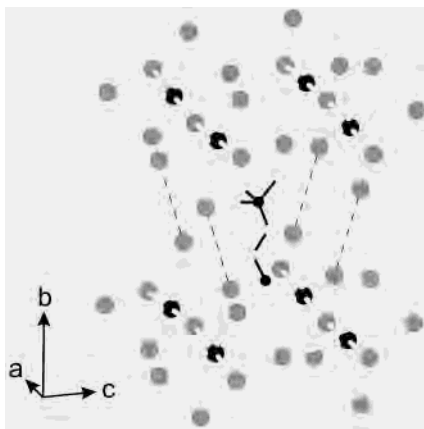


Figure 3. The cavity and the included TMAEA dication in **1**: I, large gray spheres; Sn, large black spheres; C, small open spheres; N, small black spheres. Dashed lines show the short I...I contacts. For clarity, disordering of the (CH₃)₃N⁺ group is omitted.

narrower part of the cavity. Such distortions of the Sn–I bonds develop into a regular undulating feature in the infinite framework, which is also closely complemented by the overall packing of the organic cations (Figure 2). The primary ammonium group interacts with the iodine atoms through ionic hydrogen bonding, as is indicated by the significant N...I contacts [3.85(1) Å for the apical iodine atoms, 3.71(1) Å and 3.81(1) Å for the basal ones]. Such N...I distances are slightly longer than those typically found in similar strictly primary-ammonium-based systems (see Supporting Information Table S1).

The inorganic framework of **1** exhibits interesting bonding features in comparison with the perovskite sheets of other SnI₄²⁻-based hybrid systems.²⁹ In **1**, two fairly large bond angles (162.3° and 171.5°) are observed for the bridging Sn–I–Sn units. Note that, in single-layered perovskites templated by primary amines, smaller Sn–I–Sn bond angles (under 160°) are generally observed (perhaps related to stronger hydrogen bonding in these systems),¹⁷ although significantly larger Sn–I–Sn angles have also been reported in an imidazolium-templated system.²¹ Additionally, the “straightened” Sn–I–Sn units in **1** elongate the distances between two adjacent Sn atoms and thereby expand the basal area (namely, the square-like area enclosed by the four neighboring Sn–I–Sn groups) of the cavity in Figure 3, thus making it better suited for containing the bulky trimethylammonio group.

Our recent study has shown that larger Sn–I–Sn bond angles generally correlate with narrower band gaps of the hybrid perovskite solids (Table S2 in Supporting Information).^{16,17} In this regard, the enlarged Sn–I–Sn angles in the current compound track with the shift of its exciton peak toward lower energy (indicating a smaller band gap, as mentioned above), as is indicated in the optical absorption spectrum of Figure 1. Other structural features of this compound may also be related to the smaller band gap. First, the SnI₆ unit shows only slight distortion from the ideal octahedral geometry, as can be seen from the bond lengths and angles in Table 1, indicating minimal stereochemical activity of 5s lone-pair electrons on the Sn atom. The reduced lone-pair stereoactivity in **1** is consistent with the reduced

Table 1. Selected Bond Distances (Å) and Angles (deg) for **1**

Sn–I(1)	3.1269(6)	I(1) ^a –Sn–I(2) ^a	90.57(2)
Sn–I(1) ^a	3.1269(6)	I(1)–Sn–I(2) ^a	89.43(2)
Sn–I(2)	3.1591(3)	I(2)–Sn–I(2) ^a	180
Sn–I(2) ^a	3.1591(3)	I(1) ^a –Sn–I(3)	92.34(2)
Sn–I(3)	3.1639(3)	I(1)–Sn–I(3)	87.66(2)
Sn–I(3) ^a	3.1639(3)	I(2)–Sn–I(3)	90.20(2)
		I(2) ^a –Sn–I(3)	89.80(2)
Sn–I(2)–Sn ^b	171.50(4)	I(1) ^a –Sn–I(3) ^a	87.66(2)
Sn–I(3)–Sn ^c	162.29(4)	I(1)–Sn–I(3) ^a	92.34(2)
I(1)–Sn–I(1) ^a	180	I(2)–Sn–I(3) ^a	89.80(2)
I(2)–Sn–I(1) ^a	89.43(2)	I(2) ^a –Sn–I(3) ^a	90.20(2)
I(1)–Sn–I(2)	90.57(2)	I(3)–Sn–I(3) ^a	180

^a $-x + 0.5, -y + 0.5, -z$. ^b $x - 0.5, -y + 0.5, -z$. ^c $-x + 0.5, y, -z + 0.5$.

band gap observed, because, as is mentioned elsewhere,³⁰ weakening of the lone-pair stereoactivity often associates with the population of an empty low-lying energy band in the solid by the nonbonding electrons. Second, the significant iodine–iodine interaction mentioned above should provide a path to stronger electronic coupling among the inorganic sheets, thereby perhaps helping to reduce the band gap in this compound.

To sum up, compound **1** represents a rather unique layered hybrid perovskite where a quaternary ammonium group serves as part of the templating cationic species. Optical absorption study on **1** indicates a band gap that is significantly reduced as compared with other similar compounds. The narrower band gap appears to be associated with a number of unusual attributes in the crystal structure, namely, the enlarged Sn–I–Sn bond angles, the stereochemical inactivity of the lone-pair electrons, and the interlayer electronic coupling through the close I...I contacts. The narrower band gap of **1** offers new opportunities to study and to possibly improve the charge carrier mobility and other semiconductive properties (e.g., electroluminescence^{31,32}). In addition, a congener of **1**, [(CH₃)₃NCH₂CH₂CH₂NH₃]⁺SnI₄, has been recently structurally characterized [*Pmma*, $a = 12.650(1)$ Å, $b = 12.652(1)$ Å, and $c = 10.691(1)$ Å, $Z = 5$].³³ Despite the longer dication, the overall layered perovskite structure was retained, demonstrating the more general nature of this family of hybrids templated by primary/quaternary ammonium cations.

Supporting Information Available: Full crystallographic data in CIF format for **1**. A table of N...I distances in SnI₄-based layered perovskites. A table of exciton energies, Sn–I–Sn bond angles, and Sn–I average bond lengths in SnI₄-based layered perovskites. An X-ray diffraction pattern for thin films of (PEA)₂SnI₄. X-ray diffraction patterns for powder and thin film samples of **1**. UV–vis data showing the air sensitivity of the thin films of **1**. This material is available free of charge via the Internet at <http://pubs.acs.org>.

IC0261981

(29) We have obtained about a dozen crystal structures of the formula (RNH₃)₂SnI₄ (R = organic groups), where single-layered perovskite sheets are templated by various organic cations. See refs 16 and 17 for some examples.

(30) Donaldson, J. D.; Grimes, S. M. *Rev. Silicon, Germanium, Tin Lead Compd.* **1984**, 8, 1.

(31) Gebauer, T.; Schmid, G. *Z. Anorg. Allg. Chem.* **1999**, 625, 1124.

(32) Chondroudis, K.; Mitzi, D. B. *Chem. Mater.* **1999**, 11, 3028.

(33) Xu, Z.; Mitzi, D. B., unpublished work.